Journal of Neuroscience Research 77:192–204 (2004)

Reevaluation of In Vitro Differentiation Protocols for Bone Marrow Stromal Cells: Disruption of Actin Cytoskeleton Induces Rapid Morphological Changes and Mimics Neuronal Phenotype

Birgit Neuhuber,[1] Gianluca Gallo,[1] Linda Howard,[2] Lisa Kostura,[2] Alastair Mackay,[2] and Itzhak Fischer[1]★

[1]Department of Neurobiology and Anatomy, Drexel University College of Medicine, Philadelphia, Pennsylvania
[2]Osiris Therapeutics, Inc., Baltimore, Maryland

Bone marrow stromal cells (MSC), which represent a population of multipotential mesenchymal stem cells, have been reported to undergo rapid and robust transformation into neuron-like phenotypes in vitro following treatment with chemical induction medium including dimethyl sulfoxide (DMSO; Woodbury et al. [2002] J. Neurosci. Res. 96:908). In this study, we confirmed the ability of cultured rat MSC to undergo in vitro osteogenesis, chondrogenesis, and adipogenesis, demonstrating differentiation of these cells to three mesenchymal cell fates. We then evaluated the potential for in vitro neuronal differentiation of these MSC, finding that changes in morphology upon addition of the chemical induction medium were caused by rapid disruption of the actin cytoskeleton. Retraction of the cytoplasm left behind long processes, which, although strikingly resembling neurites, showed essentially no motility and no further elaboration during time-lapse studies. Similar neurite-like processes were induced by treating MSC with DMSO only or with actin filament-depolymerizing agents. Although process formation was accompanied by rapid expression of some neuronal and glial markers, the absence of other essential neuronal proteins pointed toward aberrantly induced gene expression rather than toward a sequence of gene expression as is required for neurogenesis. Moreover, rat dermal fibroblasts responded to neuronal induction by forming similar processes and expressing similar markers. These studies do not rule out the possibility that MSC can differentiate into neurons; however, we do want to caution that in vitro differentiation protocols may have unexpected, misleading effects. A dissection of molecular signaling and commitment events may be necessary to verify the ability of MSC transdifferentiation to neuronal lineages.

Key words: neuronal differentiation; bone marrow; mesenchymal stem cell; multipotential; transdifferentiation

Marrow stromal cells (MSC) represent a population of multipotential mesenchymal stem cells distinct from hematopoietic stem cells (HSC) in the adult bone marrow. MSC contribute to regeneration of multiple tissues, including bone, cartilage, and fat. Recent studies showed that a small percentage of transplanted MSC can differentiate into neurons and glia in the uninjured brain (Kopen et al., 1999) as well as in the injured brain, where MSC transplantation may improve recovery after stroke or traumatic brain injury (Chopp and Li, 2002) and spinal cord injury (Akiyama et al., 2002; Chopp and Li, 2002; Hofstetter et al., 2002). The relative contributions of MSC transdifferentiation, contamination with other cells, and donor cell fusion with host cells remain the subjects of lively debate (for review see Herzog et al., 2003).

Because MSC are attractive candidates for cell therapies, their transdifferentiation potential in vitro has been the subject of numerous studies. Regimens for transformation to neural lineages have relied on exposure of cells to retinoic acid (RA) and cytokine cocktails (Sanchez-Ramos et al., 2000; Kim et al., 2002), butylated hydroxyanisole (BHA), and dimethyl sulfoxide (DMSO; Woodbury et al., 2000, 2002), or agents that elevate intracellular cAMP levels (Deng et al., 2001). The number of cells reported to convert from fibroblastic to neural morphology ranged from 0.5% to more than 50%. Adoption of a neuronal or glial morphology was accompanied by expres-

Contract grant sponsor: National Institutes of Health; Contract grant number: NS24707; Contract grant number: NS43882; Contract grant number: NS37515.

★Correspondence to: Itzhak Fischer, PhD, Department of Neurobiology and Anatomy, Drexel University College of Medicine, 2900 Queen Lane, Philadelphia, PA 19129. E-mail: itzhak.fischer@drexel.edu

Received 10 December 2003; Revised 1 March 2004; Accepted 9 March 2004

Published online 20 May 2004 in Wiley InterScience (www.interscience.wiley.com). DOI: 10.1002/jnr.20147

sion of neuronal or glial markers, such as neuron-specific enolase (NSE), NeuN, neurofilament M (NF-M), tau, and glial fibrillary acidic protein (GFAP). Neuronal differentiation was reported to occur without requiring passage through the cell cycle, insofar as neuron-like cells have been reported in the absence of cell division (Munoz-Elias et al., 2003). Kohyama and colleagues (2001) reported calcium uptake in response to a depolarizing stimulus after treating MSC with 5-azacytidine and transfecting them with noggin.

Patterns of gene expression of cultured MSC have been the subject of a number of studies. Such cells appear to express mesodermal, endodermal, ectodermal, and germline genes (Tremain et al., 2001; Woodbury et al., 2002; Seshi et al., 2003), suggesting the potential to differentiate into all these cell types. Interestingly, expression of many of the neural lineage-marking proteins (NSE, NF-M, NeuN, and GFAP) has also been detected in undifferentiated MSC (for review see Corti et al., 2003).

There is no generally accepted method for isolating and culturing MSC or for determining the properties and the extent of heterogeneity of the expanded cell population. Reyes and Verfaillie (2001) and Jiang et al. (2002) have reported the existence of a distinct and rare subpopulation of MSC that they have named *multipotent adult progenitor cells* (MAPC). Such cells seem able to assume mesodermal, neuroectodermal, or endodermal fates. MAPC-derived neuronal cells displayed spiking behavior, suggesting the presence of functional voltage-gated sodium channels (Jiang et al., 2003). The origin and relationship of MAPC to other cells derived from marrow stroma remains indeterminate at this time.

Because MSC isolation, purification, culture expansion, and characterization are variable, the validity of neuronal transdifferentiation has been hard to assess. In particular, 1) does in vitro neuronal differentiation of MSC yield true neurons or merely morphological artifacts? 2) If transdifferentiation events are possible are they restricted to a subpopulation of MSC? 3) Is this subpopulation representative of a more primitive and pluripotent stem cell than the MSC as generally envisioned?

In this study, we reevaluated an in vitro differentiation process, in which MSC undergo rapid transformation into neuron-like phenotypes following treatment with a chemical induction medium containing DMSO (Woodbury et al., 2000, 2002). We found that, with this protocol, formation of neurite-like processes was a result of cytoplasm retraction caused by F-actin depolymerization, not by microtubule-mediated extension. Although we confirmed the display of neuron- and glia-specific antigens by induced cells, such expression was incomplete for a true neuronal phenotype and to some extent was observed in naïve MSC. Furthermore, fibroblasts were capable of forming similar processes through cytoplasmic retraction. These results do not rule out a possible potential of MSC to differentiate into neurons, but show that differentiation protocols may have misleading morphological effects. Critical examination of the differentiation process is necessary to determine the validity of the neuronal phenotype.

MATERIALS AND METHODS

Isolation of Rat MSC

MSC were cultured from bone marrow of 10-week-old transgenic Fisher rats (Mujtaba et al., 2002) as previously described (Lennon et al., 1995). After euthanasia, marrow was flushed with Hank's buffered saline solution, pooled, and counted. After centrifugation (600*g*, 10 min), cells were plated at 120×10^6 cells/cm^2 in 10% fetal bovine serum (Hyclone, Logan, UT), 45% Ham's F-12 (Invitrogen, Carlsbad, CA), 45% α-MEM (Invitrogen), supplemented with antibiotics (100 U/ml penicillin G and 100 μg/ml streptomycin sulfate; Invitrogen). Flasks were incubated in a humidified atmosphere with 5% CO_2 at 37°C. After 8 days, nonadherent cells were removed, and remaining cells detached with 0.05% trypsin/0.53 mM EDTA (Invitrogen) and replated at 2,000 cells/cm^2. Subsequently, cultures were passaged at 4-day intervals.

Differentiation of Rat MSC Into Mesenchymal Lineages

Adipogenesis. MSC were seeded into six-well plates at 20,000 cells/cm^2 and cultured in growth medium until confluent. Cultures were then placed in adipogenic induction medium [DMEM with 4.5 mg/ml glucose (Invitrogen), 10% fetal bovine serum (FBS), and antibiotics as described, with 0.5 mM methylisobutylxanthine, 1 μM dexamethasone, 10 μg/ml insulin, and 100 mM indomethacin (all from Sigma, St. Louis, MO)] for 3 days and subsequently moved to adipogenic maintenance medium [DMEM with 4.5 mg/ml glucose (Invitrogen), 10% FBS, antibiotics, and 10 μg/ml insulin (Sigma; Pittenger et al., 1999)] for 1 day. After three cycles, cells were kept in maintenance medium for 7 days and fixed with 4% paraformaldehyde. Staining with oil red O facilitated microscopic evaluation of the accumulation of neutral lipids.

Osteogenesis. MSC were seeded in six-well dishes at 3,000 cells/cm^2. After 2 days, growth medium was replaced by osteogenic medium (growth medium supplemented with 100 nM dexamethasone (Sigma), 50 μM ascorbate-2-phosphate (Wako Pure Chemicals, Chuo-ku, Osaka, Japan), and 10 mM β-glycerol phosphate (Sigma). Medium was replaced twice weekly. After 18 days, medium was aspirated, and cells were solubilized in 1 N HCl. Acid-soluble calcium was determined colorimetrically (Sigma 587-M). An additional well was stained by using the von Kossa method to visualize calcium phosphate deposition (Pittenger et al., 1999).

Chondrogenesis. Conditions promoting human MSC chondrogenesis (Mackay et al., 1998) did not promote differentiation of rat MSC (data not shown). Instead, 500,000 rat MSC were pelleted (600*g*) in a 15-ml polypropylene tube in high-glucose DMEM (Invitrogen) with 1% FBS (Hyclone), antibiotics, 50 μg/ml ascorbate 2-phosphate, 40 μg/ml proline, 2 mM pyruvate (Invitrogen), ITS$^+$ (Collaborative Research, Bedford, MA; final concentrations 6.25 μg/ml insulin, 6.25 μg/ml transferrin, 6.25 μg/ml selenous acid, 5.33 μg/ml linoleic acid, and 1.25 mg/ml bovine serum albumin), 100 nM dexamethasone, 10 ng/ml transforming growth factor-β3 (TGF-β3; R&D Systems, Minneapolis, MN), and 200 ng/ml

recombinant bone morphogenic protein-2 (BMP-2; R&D Systems). Medium was changed three times per week. On day 21, pellets were fixed in 4% paraformaldehyde, embedded in paraffin, and sectioned (5 μm). Multiple sections were stained with safranin O for detection of anionic proteoglycans and with a monoclonal anticollagen II antibody (C4F6; generous gift of Dr. Chichester, University of Rhode Island). Primary rat dermal fibroblasts failed to demonstrate osteogenic, chondrogenic, or adipogenic differentiation in these assays (data not shown).

Cell Culture

MSC from passage 2 were plated on plastic dishes at a density of 2,000/cm^2 and cultured in 45% Ham's F12 and 45% α-MEM (both from Invitrogen) supplemented with 10% FBS (Hyclone) and 1% penicillin and streptomycin (Invitrogen). For selected experiments, MSC were plated on dishes coated with 25 μg/ml laminin (Invitrogen).

Rat dermal fibroblasts were isolated from neonate rats as described by Koksoy et al. (2001). Cells from passages no higher than P8 were plated on plastic dishes at a density of 2,000/cm^2 and cultured in α-MEM supplemented with 10% FBS and 2 mM L-glutamine (Cellgro, Herndon, VA). Cells were maintained at 37°C and 5% CO_2.

Induction Protocols and Drug Treatments

Induction for neuronal differentiation was performed as previously described by Woodbury and colleagues (2002). Briefly, MSC and fibroblast cultures were grown overnight to a density of about 30% in their respective media, followed by a 24-hr incubation in preinduction medium consisting of 40% Ham's F12 and 40% α-MEM, 20% FBS, and 10 ng/ml basic fibroblast growth factor (bFGF; PreproTech Inc., Rocky Hill, NJ). After being rinsed with phosphate-buffered saline (PBS), cells were incubated at 31°C in induction medium [49% Ham's F12 and 49% α-MEM, 2% DMSO, 100 μM BHA, 10 μM forskolin, 2 mM valproic acid, 5 U/ml heparin (all from Sigma), 5 nM K252a (Calbiochem, La Jolla, CA), 25 mM KCl, 1xN2 supplement (Invitrogen), 10 ng/ml platelet-derived growth factor (Upstate Biotechnologies, Lake Placid, NY), and 10 ng/ml bFGF] for 24 hr. For reversion studies, induction medium was replaced by MSC or fibroblast medium after 24 hr. For DMSO treatment, MSC or fibroblast cultures were incubated in 49% Ham's F12 and 49% α-MEM containing 2% DMSO for 24 hr.

Disruption of the actin cytoskeleton was achieved by adding 2 μg/ml cytochalasin-D (Cyto-D; Sigma) or 2 μM/ml latrunculin-A (Lat-A; Molecular Probes, Eugene, OR) to the medium of MSC or fibroblast cultures. Depolarization of microtubules was induced by adding 10 μM/ml nocodazole (Sigma). After 90 min, cells were fixed and immunostained as described below.

Time-lapse studies were performed with a 135 Axiovert microscope (Carl Zeiss Inc., Thornwood, NY) using a ×20 phase objective and Axiovision (Zeiss) software. The stage was kept at 31°C by using an air-curtain incubator. Images were taken at 2-min intervals for the first 90 min of exposure of MSC and fibroblast cultures to induction medium. A second 90-min sequence was taken 24 hr after induction of MSC cultures. A third sequence from an MSC culture in preinduction medium served as a control.

Immunocytochemistry and Quantification

For immunostaining, cells were fixed in 4% paraformaldehyde after 24 hr in induction medium, washed with PBS, and blocked in 10% normal goat serum (NGS; Invitrogen) for 1 hr. Primary and secondary antibodies were incubated for 1 hr at room temperature. Primary antibodies used in this study were polyclonal antineurofilament M (Chemicon, Temecula, CA; 1:200), polyclonal antitau (Black et al., 1996; 1:1,000), monoclonal anti-βIII-tubulin (Babco, Richmond, CA; 1:500), monoclonal antisynaptophysin (Chemicon; 1:200), polyclonal anti-GFAP (Dako, Carpinteria, CA; 1:500), monoclonal antivimentin (Developmental Studies Hybridoma Bank, Iowa City, IA; 1:20), and monoclonal antinestin (PharMingen, San Diego, CA; 1:1,000). Titers for each antibody were established with cells known to express its antigen. Control reactions with the primary antibody omitted were routinely performed. In addition, absence of staining was confirmed in controls in which primary antibodies were replaced with corresponding immunoglobins at the same concentration as the primary antibodies (pure rabbit and mouse IgG, whole molecule; Jackson Immunoresearch, West Grove, PA). Biotinylated secondary antibodies were obtained from Jackson Immunoresearch and used at a dilution of 1:200. The Elite Vectastain ABC kit (Vector Laboratories, Burlingame, CA) and Fast Diaminobenzidine (DAB) Tablet kit (Sigma) were used according to manufacturers' suggestions to develop the staining.

Cells were photographed under phase optics (×20 objective) with an Olympus CK40 microscope connected to a Nikon Coolpix 990 digital camera. For quantification, cells in 20 randomly selected fields were counted with a ×10 objective. Cells with refractile cell bodies and extended processes (neuron-like cells) were calculated as a percentage of the total cell count.

To label cytoskeletal proteins, cells were fixed in 0.25% glutaraldehyde in PHEM buffer (Black et al., 1996) for 15 min, thereby removing soluble tubulin. Subsequently, cells were incubated in 2 mg/ml sodium borohydride for 15 min, washed with PBS, and blocked in 10% NGS. Cells were then incubated in antitubulin-FITC (Sigma; 1:100) for 1 hr and in phalloidin-RITC (Molecular Probes; 5 μl/100 ml) for 30 min. A 200M Axiovert microscope (Zeiss) with a ×20 objective and Axiovision imaging software was used to evaluate the cells.

Reverse Transcription-Polymerase Chain Reaction

RNA was isolated from control MSC or fibroblast cultures or cultures that had been treated with induction medium for 24 hr using the Purescript RNA isolation kit (Gentra Systems, Minneapolis, MN). Contaminating genomic DNA was removed using the DNA-free kit (Ambion, Austin, TX). Quantitative reverse transcription-polymerase chain reaction (RT-PCR) was performed on a Roche LightCycler (Roche, Indianapolis, IN) by using the QuantiTect SYBR Green RT-PCR Kit (Qiagen, Valencia, CA) with primers at a concentration of 0.5 μM (βIII-tubulin: 5′-GGCCTCCTCTCACAAGTATGT-3′ and 5′-CGCCCTCTGTATAGTGC-3′; NF-M: 5′-AGGAGCGCCACAACCACGACC-3′ and 5′-ATGCGGCGATCTCGATGTCCA-3′; and vimentin: 5′-TGTCCGCCAGCAGTATGA-3′ and 5′-CCTGTCTCCGGTATTCGTTTG-3′). In each reaction, 100 ng of total RNA were used as a template. Water was used as a

negative control; 20 ng or 1 ng poly-A rat brain RNA (BD Biosciences, Palo Alto, CA) was used as a positive control. Reaction conditions were as follows: 1 cycle 50°C, 20 min; 1 cycle 95°C, 15 min; 40 cycles 95°C, 0 sec; 55°C, 10 sec; 72°C, 10 sec with a single data acquisition. After amplification, a melting analysis was performed with a transition from 60°C to 95°C at 0.1°C/sec with continuous data acquisition. Transcript levels were quantified by comparison with the signal from cDNA standards run at the same time as the samples; the concentration of these standards ranged from 1–1,000,000 copies per PCR. cDNA standards were prepared from PCR product purified from agarose gel slices with the GFX Kit (Amersham Bioscience, Arlington Heights, IL). The concentration of the purified PCR product was determined by using the PicoGreen dsDNA quantitation kit (Molecular Probes); PCR product was diluted in dilution buffer (1 mM Tris-HCl, pH 8.0, 0.1 mM EDTA containing 10 ng/μl yeast tRNA) to give a concentration of 10^5 copies/μl, and further tenfold dilutions of this stock were prepared and all cDNA standard solutions stored in siliconized tubes. Standards were run in duplicate with 2 μl per reaction. Samples were run in triplicate with 2 μl per reaction.

RESULTS

Differentiation Potential of Rat MSC

To confirm the multipotential mesenchymal properties of rat MSC, we assayed for adipogenesis, osteogenesis, and chondrogenesis in vitro. The assays as performed did not induce dermal fibroblasts to undergo these phenotypic alterations. Adipogenic MSC formed phase-bright vacuoles that stained red with oil red O (Fig. 1A). MSC cultured under osteogenic conditions deposited an average of 30 μg calcium per well, whereas control MSC deposited less than 11 μg (data not shown). Only osteogenic MSC were positive for von Kossa staining (Fig. 1B). Micromass pellets of MSC responded to chondrogenic conditions by accumulating type II collagen (Fig. 1C) and anionic proteoglycans in the extracellular matrix (Fig. 1D).

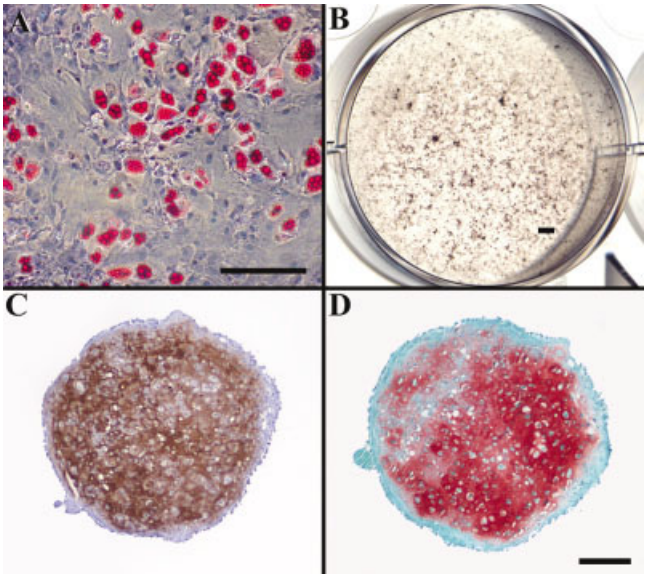

Fig. 1. In vitro assays demonstrate the multipotency of rat MSC. After primary culture, cells were assayed for adipogenesis, osteogenesis, and chondrogenesis. MSC developed lipid vesicles (red) in dense monolayer cultures when treated with adipogenic supplements (**A**). MSC plated sparsely in a 35-mm well deposited calcium phosphate (marked black with von Kossa stain) in the extracellular matrix under osteogenic conditions (**B**). Immunohistochemistry revealed that MSC at the conclusion of an additional round of expansion expressed type II collagen throughout the extracellular matrix of the micromass pellet after 21 days (**C**). Safranin O staining revealed extensive deposition of anionic proteoglycans (**D**). Scale bar in A = 50 μm; bar in B = 2 mm; bar in D = 200 μm for C,D.

Morphological Changes of MSC After Neuronal Induction

Untreated and preinduced cultures of rat MSC consisted predominantly of spindle-shaped cells and few large, flat cells (Fig. 2A,B). Within 2 hr after addition of induction medium, 73% of MSC (n = 511) had changed their morphology and adopted neuronal- or glial-like phenotypes, distinguished by highly refractile cell bodies with neurite-like processes terminating in structures resembling growth cones (Fig. 2C). This finding is similar to findings previously described (Sanchez-Ramos et al., 2000; Woodbury et al., 2000, 2002; Deng et al., 2001; Kim et al., 2002). No additional changes in morphology were observed 24 hr after induction (Fig. 2D). In highly refractile cells, the region bounded by process tips was reminiscent of the cell shape of untreated MSC, and some of the less-refractile cells were intermediate in shape between untreated and neuron-like MSC (see Fig. 2C, long arrow). These findings suggested that the neuron-like morphology might be caused by retraction of cytoplasm rather than active process extension. The change in morphology could be reversed by returning MSC cultures to MSC medium as previously described (Woodbury et al., 2002). Within 1 hr, most cells had reverted to their original shape (Fig. 2E), a finding inconsistent with changes expected for terminal differentiation. All experiments were repeated with human MSC and similar results obtained (data not shown).

DMSO is a major component of the induction medium. To examine its effects on MSC, we incubated MSC directly without preincubation, in serum-free medium with 2% DMSO. Within 1 hr of application, most cells displayed a neuron-like morphology (Fig. 2F). This effect was reversible by returning the cells to MSC medium.

Induction of Fibroblasts Results in the Acquisition of a Neuron-Like Morphology

To investigate whether the effects of induction medium were limited to stem cells, we subjected rat dermal fibroblasts to the same protocol. We observed large, flat cells in untreated and preinduced cultures (Fig. 3A,B). Addition of induction medium caused cytoplasmic retraction in 76% (n = 884) of the cells (Fig. 3C,D), resulting in a neuron-like phenotype with refractile cell bodies and long, extended processes with structures resembling growth cones at the tips. Thus, the induction medium affected differentiated cells and stem cells in a similar way.

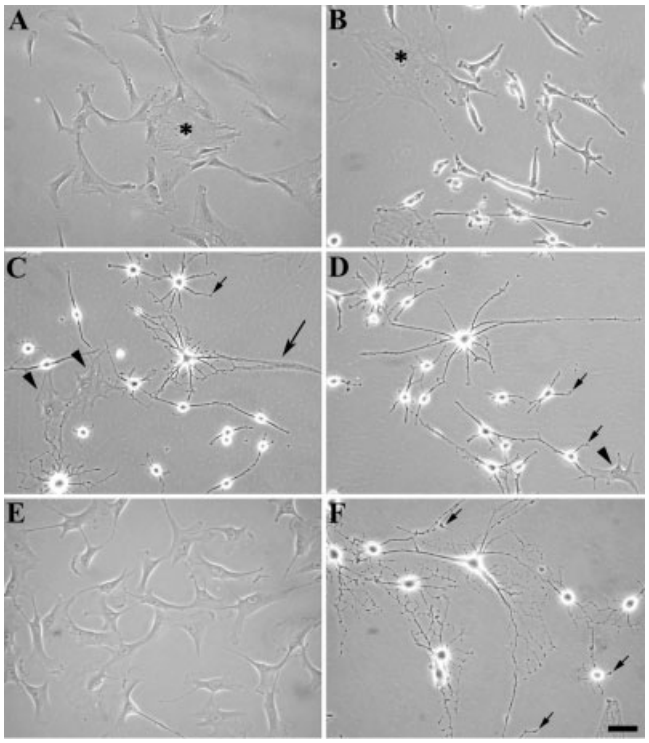

Fig. 2. MSC assume a neuron-like morphology upon treatment with induction medium. MSC cultures before treatment (**A**) and after preincubation (**B**) consist of spindle-shaped cells and flat cells (asterisks). Addition of induction medium results in adaptation of a neuron-like morphology, with highly refractile cell bodies and thin extended processes, which terminate in structures resembling growth cones (short arrows; **C,D**). Some cells have an intermediate morphology, with wide processes (long arrow; C); other cells retain their preinduction morphology (arrowheads). Images were taken 2 hr (C) and 24 hr (D) after addition of induction medium. Morphological changes are reversible by reintroduction of MSC medium (**E**). Treatment of MSC cultures with 2% DMSO causes similar changes in cell morphology (arrows indicate growth cone-like structures; **F**). Scale bar = 50 μm.

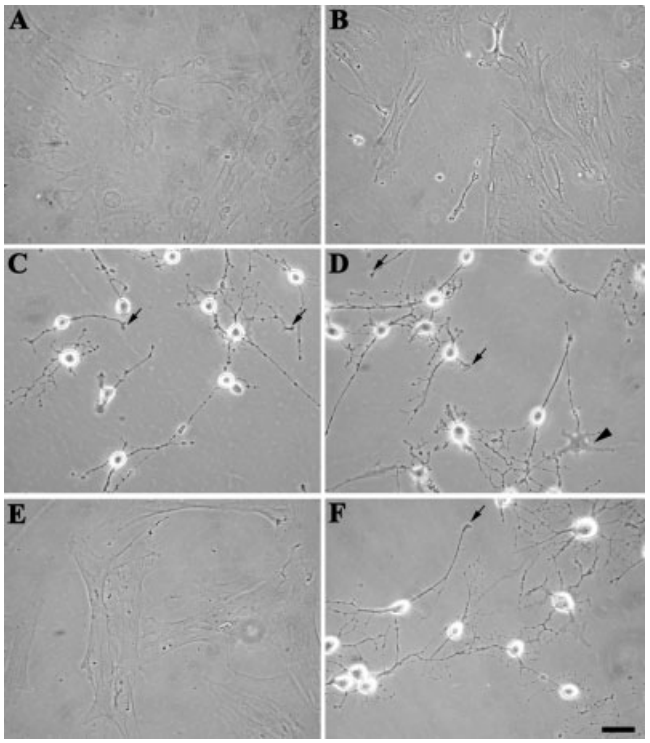

Fig. 3. Fibroblasts adopt similar neuron-like morphologies upon treatment with induction medium. Fibroblast cultures before treatment (**A**) and after incubation in preinduction medium (**B**). Addition of induction medium causes morphological changes similar to those in MSC, with highly refractile cell bodies and thin extended processes, which terminate in structures resembling growth cones (arrows; **C,D**). Some cells show an intermediate phenotype (arrowhead). Images were taken 2 hr (C) and 24 hr (D) after addition of induction medium. Morphological changes are reversible by reintroduction of fibroblast medium (**E**). Treatment of fibroblast cultures with 2% DMSO also induces neuron-like morphology similarly to addition of induction medium (arrow indicates growth cone-like structure; **F**). Scale bar = 50 μm.

The onset of morphological changes was as fast in fibroblasts as in MSC cultures. As with MSC, this process was reversible by returning the cells to their original growth medium (Fig. 3E). Fibroblasts also adopted neuronal morphologies upon addition of 2% DMSO alone (Fig. 3F).

Time-Lapse Analysis of Morphological Changes During Neuronal Induction

We used time-lapse phase-contrast microscopy to study the dynamics of morphological changes during neuronal induction. Within 90 min of the initiation of induction, 73% of visualized cells (n = 26) assumed a neuron-like morphology, defined as the appearance of a spherical cell body with multiple processes (Fig. 4A–C). The mean time cells took to undergo this transition was 40 ± 5 min (mean ± SD). Morphological changes occurred because most of the cell edge retracted toward the nucleus. Some regions of the cell edge did not retract, resulting in the formation of processes emanating from the center of the cell. Thus, processes formed through retraction of the surrounding cytoplasm, not through process extension, as is the case with process outgrowth in neurons. Similar changes in morphology were observed in induced fibroblast cultures (Fig. 4D–F).

Neuronal growth cones are motile and extend along processes and at their tips. To determine whether processes formed by induced MSC were capable of similar extension, we monitored the behavior of process tips during induction, and 24 hr later. We did not observe process extension at either time point.

Because neurons fail to grow on untreated plastic surfaces, we wondered whether process elaboration by induced MSC might be promoted on laminin-coated dishes. Changes in MSC morphology after addition of induction medium were comparable to those seen with MSC grown on plastic, except that retraction of the cytoplasm was not as prominent. This was, presumably, a

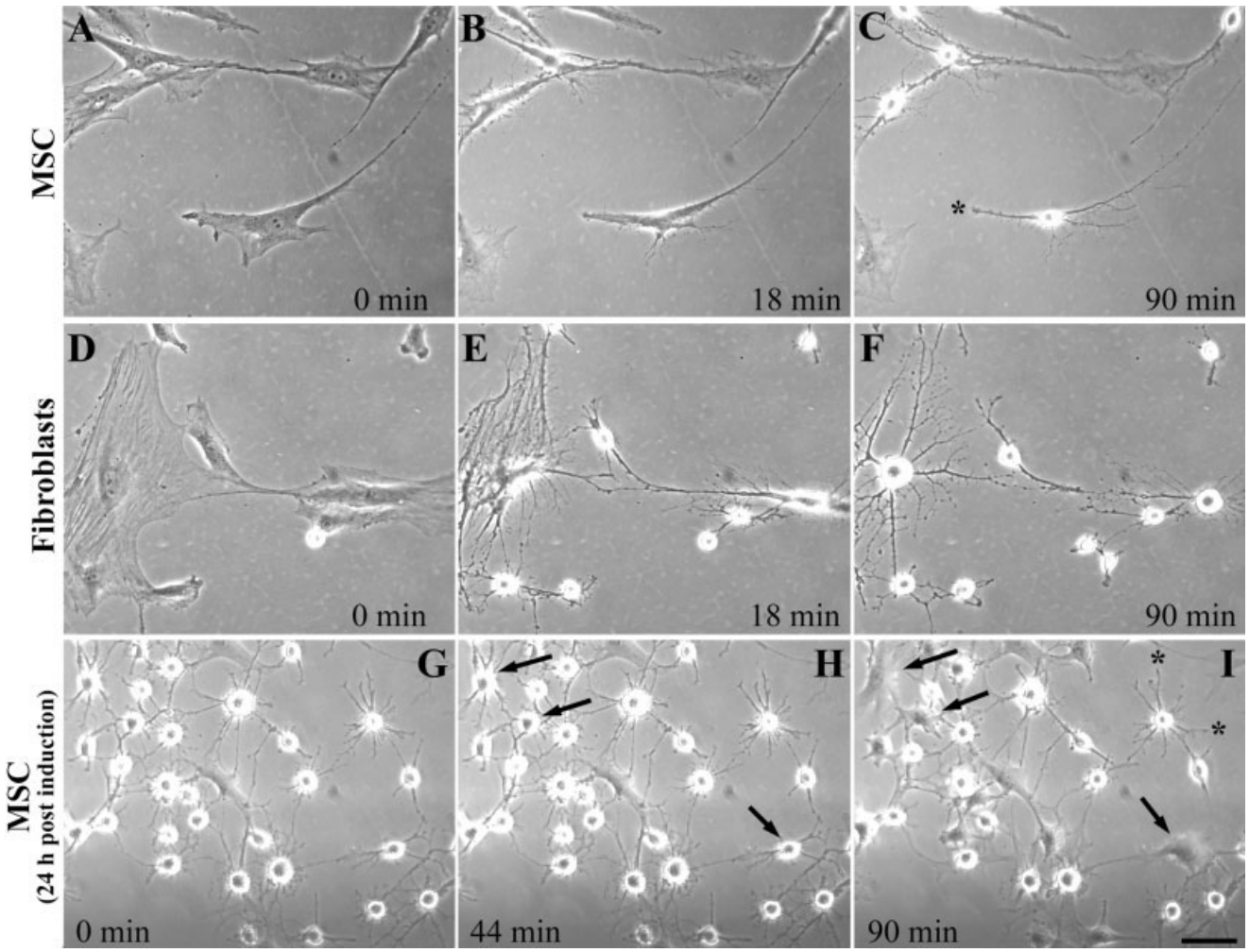

Fig. 4. Time-lapse imaging reveals that acquisition of neuron-like morphology is due to retraction of the cell edge. During the first 90 min following induction, MSC (**A–C**) and fibroblasts (**D–F**) retract the majority of their cell edges while retaining some adhesions to the substrate, resulting in the formation of long, neurite-like processes terminating in growth cone-like structures (asterisk). Time-lapse imaging of MSC 24 hr after induction revealed no significant mobility of these processes. Certain MSC were seen to revert back to preinduction morphology (**G–I**; arrows point to cells that reverted to a preinduction morphology). Scale bar = 50 μm.

result of better adhesion of cells to the laminin substrate. However, laminin did not promote any significant process outgrowth after the initial acquisition of the neuronal phenotype (data not shown).

We observed, in the time-lapse videos of MSC cultures induced for 24 hr, that 31% of cells (n = 35) with neuronal morphology spontaneously reversed their changes to a neuronal morphology and returned to the spread shape that characterizes undifferentiated MSC (Fig. 4G–I). Such reversal of morphology occurred when edges of the cell protruded to refill the spaces between processes. The reversal from neuron-like to MSC morphology occurred over 20–30 min. These observations demonstrate that neuron-like MSC retain the ability to protrude the cell edge but do so rarely and always within the original cell boundaries.

To investigate whether the nonuniform retraction of the cell edge was due to stronger adhesion of some areas of the cell to the plastic growth surface, we immunostained uninduced and induced MSC cultures with antibodies against paxillin, a constituent of focal adhesions. Paxillin-positive patches were present throughout the cell periphery in uninduced MSC (Fig. 5A). In induced MSC, diffuse paxillin immunolabel was observed in the cytoplasm, indicating disassembly of focal adhesions; however, some paxillin-positive patches were localized alongside the processes, suggesting that strong adhesion to the substrate allowed maintenance of these extensions even when the rest of the cell edge was retracted (Fig. 5B).

Disruption of F-Actin Mimics Differentiation

We stained MSC and fibroblasts for actin filaments and microtubules. In untreated cultures, F-actin was organized as stress fibers and lamellipodial protrusions (Fig. 6A,E). Microtubules in control cultures originated near

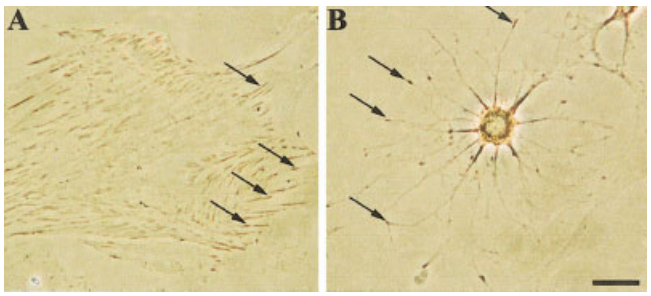

Fig. 5. Focal adhesions are localized at the tips of processes. Staining of uninduced (**A**) and 24-hr-induced MSC cultures (**B**) with antibodies against paxillin. Paxillin-positive patches (arrows), indicating focal adhesions, are present throughout the cell periphery of uninduced MSC (A). In addition to diffuse paxillin immunolabel, visible in the cytoplasm of induced MSC, paxillin-positive patches (arrows) are localized at the tips of processes. Scale bar = 25 μm.

the nucleus and extended throughout the cytoplasm (Fig. 6B,F). By 40 min after induction, the actin network became disorganized, resulting in the loss of stress fibers and lamellipodial protrusions (Fig. 6C,G). Microtubules became restricted to regions where the cell edge was not fully retracted, resulting in a microtubule array with a bundled appearance (Fig. 6D,H). Rather than being a cause, this microtubule organization is likely to be a consequence of changes in cell morphology.

The observed reorganization of F-actin following induction is similar to that seen when the F-actin network is disrupted by treatment with Cyto-D or Lat-A. Therefore, we compared the morphology and organization of F-actin and microtubules in cells treated with Cyto-D or Lat-A with those of induced MSC. Pharmacological disruption of F-actin triggered morphological changes and cytoskeletal reorganization similar to that observed during neuronal induction, causing MSC to adopt a neuron-like morphology (Fig. 7A–H). Time-lapse phase microscopy revealed that these changes again resulted from retraction of the cell edge (data not shown). Disruption of microtubules with nocodazole did not result in the acquisition of a neuron-like morphology by MSC (Fig. 7I–L).

Immunocytochemical and RT-PCR Analysis of Changes in Protein and Gene Expression Upon Induction

To investigate the effects of the induction medium on protein expression, we looked at markers for neurons (NF-M, tau, βIII-tubulin, synaptophysin), glia (GFAP), fibroblasts (vimentin), and neural progenitors (nestin) in uninduced (data not shown), preinduced, and induced MSC. Weak cytoplasmic staining for NF-M and tau was observed in 100% of uninduced and preinduced MSC (Fig. 8A,B). In neuron-like cells, immunostaining was most pronounced in the cytoplasm of the cell body and extended into the processes (Fig. 8E,F). Positive staining for βIII-tubulin was not observed in uninduced or preinduced MSC (Fig. 8C). Among induced MSC, 21% (n = 66) of neuron-like cells were βIII-tubulin positive (Fig. 8G). No immunostaining for synaptophysin (Fig. 8D,H) was observed in uninduced, preinduced, or induced MSC. No signal for GFAP was detected in uninduced and preinduced MSC (Fig. 9A), but 50% of induced MSC (n = 182) with a neuron- or glia-like phenotype strongly expressed this glial marker (Fig. 9D). Vimentin intermediate filaments were detected in all MSC (Fig. 9B,E). A subpopulation of MSC was positive for nestin in uninduced (40%), preinduced (63%), and induced (80% of neuron-like, 54% of MSC-like; Fig. 9C,F) MSC cultures. The presence of nestin and some neuronal and glial markers in induced MSC as well as decreased vimentin expression might suggest that MSC are driven toward a neuronal phenotype by exposure to induction medium. However, the absence of other neuronal markers and the expression of these proteins (NF-M, tau, βIII-tubulin, GFAP) by fibroblasts in a similar pattern (data not shown) suggest that treatment with induction medium may promote aberrant gene expression rather than an in vitro analogue of the systematic gene expression, that is seen during differentiation.

Quantitative RT-PCR analysis revealed a 1.5-fold and 11.5-fold decrease in vimentin mRNA levels upon induction of MSC and fibroblasts, respectively (Table I, Fig. 10). A 51-fold increase in NF-M mRNA expression was observed in induced vs. uninduced MSC (Table I, Fig. 10A–D). βIII-tubulin message was detected in uninduced MSC and was 14-fold increased in induced MSC (Table I, Fig. 10). We found in fibroblasts 1.9- and 1.2-fold increases in the expression of NF-M and βIII-tubulin, respectively. Thus, addition of neural induction medium leads to changes in the gene expression pattern in both MSC and fibroblasts, though to different extents. Woodbury et al. (2002) claim that these changes are due to a modulation of gene expression upon addition of neural induction medium in already "multidifferentiated" MSC. However, even if levels of βIII-tubulin and NF-M transcripts in MSC and fibroblasts increase after induction, the absolute levels are very low and are of questionable physiological relevance. In addition, the expression of a mere subset of neuronal genes and proteins in induced cells does not serve as proof for neuronal differentiation.

DISCUSSION

Changes in Cytoskeleton and Gene Expression

In this study, we have demonstrated that the adoption of a neuron-like morphology by MSC in the early stage of exposure to induction medium containing BHA and DMSO in vitro is due to a breakdown of the actin cytoskeleton and a retraction of the cell edge. The mechanism of formation of neurite-like processes in response to induction medium is thus strikingly different from the extension-based generation of axons and dendrites of neurons. Additionally, the motility and active process extension that characterize growing neurons are absent from induced MSC. This strongly suggests that the notion that MSC readily differentiate into neurons in vitro (Wood-

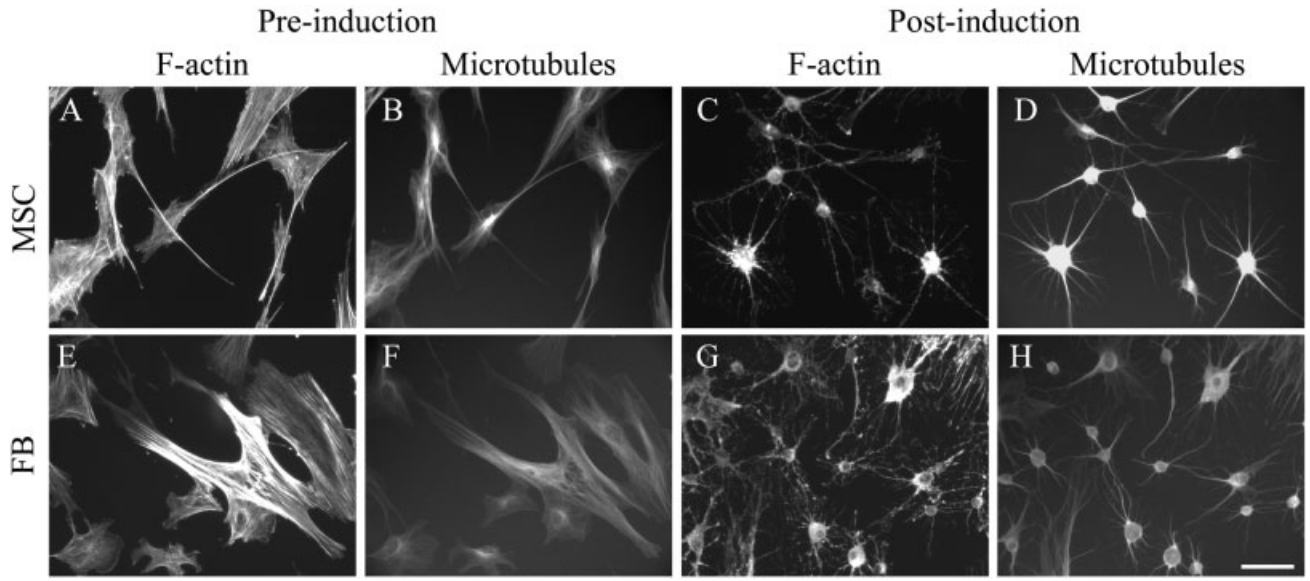

Fig. 6. Reorganization of the cytoskeleton following neuronal induction. Preinduction MSC (A,B) and fibroblasts (E,F) exhibit the typical cytoskeletal organization of flattened cells in vitro. Actin filaments are present in the form of stress fibers, long linear bundles of actin filaments, and small lamellipodia at the leading edge (**A,E**). Microtubules in preinduced MSC and fibroblasts are found throughout the cytoplasm (**B,F**). Induction of either cell type disrupts the actin cytoskeleton, resulting in filament clumping (**C,G**). Ninety minutes after induction, microtubules reorganize into bundles that fill the processes (**D,H**). Cells were fixed and stained with TRITC-phalloidin and FITC-conjugated primary antibody to tubulin to visualize actin filaments and microtubules, respectively. Scale bar = 50 μm.

bury et al., 2000, 2002) is an explanation that is incomplete at best. More likely, the adaptation of the neuronal phenotype represents an artifact. The fluctuation between neuron-like and MSC morphologies suggests that MSC have a dynamic, reversible response to induction conditions that is not characteristic of bona fide differentiation. The rapidity with which the neuron-like morphology is both gained and lost also argues against physiological differentiation. It seems unlikely that the changes in cellular organization and gene and protein expression that largely constitute commitment to differentiation could be so advanced within 45 min of exposure to inductive conditions.

The presence of a subset of neuronal markers cannot be taken to prove commitment to a neuronal fate. To clearly identify a differentiated MSC as a neuron, it should display a complete set of neuronal markers. Other features of functional neurons, such as synaptic markers and machinery, should also be confirmed. A final proof of functionality would be the identification of action potentials accompanied by synaptic neurotransmitter release. Although it has been shown previously that depolymerization of the actin cytoskeleton induces process formation in MAP2-transfected nonneuronal cells (Edson et al., 1993), process formation requires MAP2 overexpression. In addition, MAP2-dependent process formation is an active extension process, unlike the formation of neurite-like structures in MSC that develop through retraction of the cytoplasm.

Dermal fibroblasts did not differentiate into osteocytes, chondrocytes, or adipocytes; however, they assumed neuronal phenotypes just as readily as MSC when exposed to neuronal induction medium. Therefore, it seems that agents contained in the induction medium cause the breakdown of the actin cytoskeleton, creating a morphological artifact rather than inducing a physiological reprogramming event. This notion is supported by the fact that treatment of MSC and fibroblasts with 2% DMSO yielded cell phenotypes that were difficult to distinguish from those promoted by complete induction medium. In this regard, the observation by Lu, Blesch, and Tuszynski (this issue) of "pseudoneuronal" phenotypes in various cell types upon treatment with β-mercaptoethanol or DMSO is also consistent with the latter explanation.

Cellular and Molecular Effects of Chemical Agents in Induction Media

DMSO is a commonly used solvent in biological studies, even though its physiological and pharmacological effects are poorly understood. In some contexts, DMSO is a cell-differentiating agent (for review see Santos et al., 2003). Exposure to DMSO has been reported to inhibit c-myc expression (Darling et al., 1989), arrest the cell cycle in lymphoid cell lines (Sawai et al., 1990), prevent dedifferentiation of normal cells (Isom et al., 1985), and increase cAMP levels (Terasawa et al., 1981). As with RA, DMSO accelerates differentiation and induces process formation in microglial cells (Giulian and Baker, 1986). Treatment of certain neuroblastoma cell lines with 2% DMSO results in morphologically differentiated cultures with extensive process formation and electrical excitabil-

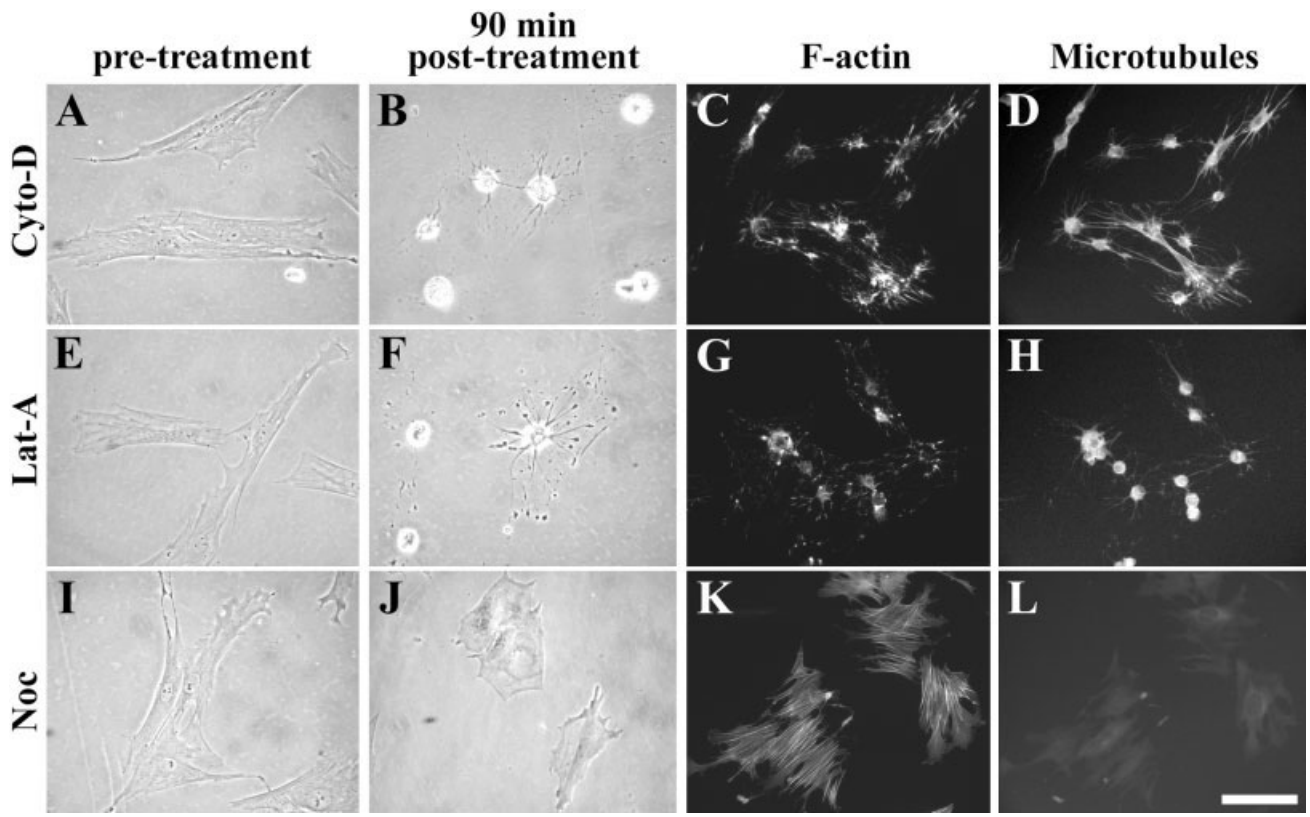

Fig. 7. Disruption of actin filaments results in neuron-like morphology. Treatment of MSC or fibroblasts with either 2 μg/ml cytochalasin D (Cyto-D) or 2 μM latrunculin-A (Lat-A) causes retraction of cell edges and results in a neuron-like morphology (**A,B,E,F**). Disruption of microtubules using 10 mM nocodazole (Noc) does not result in a neuron-like morphology (**I,J**). Cyto-D and Lat-A (**C,G**) disrupt the actin cytoskeleton, resulting in filament clumping. Noc (**K**) does not disrupt the actin cytoskeleton. In Cyto-D- and Lat-A-treated cells, microtubules reorganize into bundles that fill the cytoplasmic space (**D,H**). Noc treatment causes microtubule disruption (**L**), resulting in weak homogenous cytoplasmic staining. All images of the cytoskeleton were taken from cells fixed 90 min after treatment and stained with TRITC-phalloidin and FITC-conjugated primary antibody to tubulin to visualize actin filaments and microtubules, respectively. Scale bar = 50 μm.

ity, although these changes are not accompanied by increases in the levels of acetylcholinesterase or tyrosine hydroxylase (Kimhi et al., 1976). In contrast, embryonic carcinoma cells do not differentiate into neurons or glia but differentiate into cardiac and skeletal muscle upon treatment with DMSO (McBurney et al., 1982). Thus, a treatment that includes exposure to 2% DMSO is likely to promote changes to the morphology and gene expression patterns of the cells under consideration. These changes will not necessarily be diagnostic of the induction of an organized program. Furthermore, Lu, Blesch, and Tuszynski (this issue) show that MSC treated with Tween 20, Triton X-100, or concentrated salts or bases display morphological changes reminiscent of those described here. This strongly suggests that these agents, and DMSO, induce phenotypic changes in MSC that are unrelated to a program of neuronal differentiation.

cAMP is a ubiquitous intracellular second messenger that regulates such diverse cellular functions as Ca^{2+} influx, excitability, and gene expression. In prostate tumor cells, cAMP analogues and phosphodiesterase inhibitors can induce a neuronal phenotype, including expression of NSE (Bang et al., 1994). Forskolin, a stimulator of adenyl cyclase, can reversibly induce neuroendocrine characteristics (Cox et al., 1999). Isobutylmethylxanthine or dibutyryl cAMP treatments are also commonly used to elevate intracellular cAMP in cultured cells. Deng et al. (2001) reported that treatment of human MSC with these agents induced 25% of the cells to assume a neuron-like morphology and express NSE, but not markers of mature neurons. Elevation of cytoplasmic cAMP levels could be responsible for the changes in protein expression that were observed.

Differentiation Potential of MSC

Do MSC retain potentials that they have never exhibited during normal development, and can developmental potential be reprogrammed under specific conditions and result in transdifferentiation to nonmesenchymal phenotypes? Or is such pluripotency restricted to a subpopulation of early progenitor cells that is contained within the MSC population? Transdifferentiation is de-

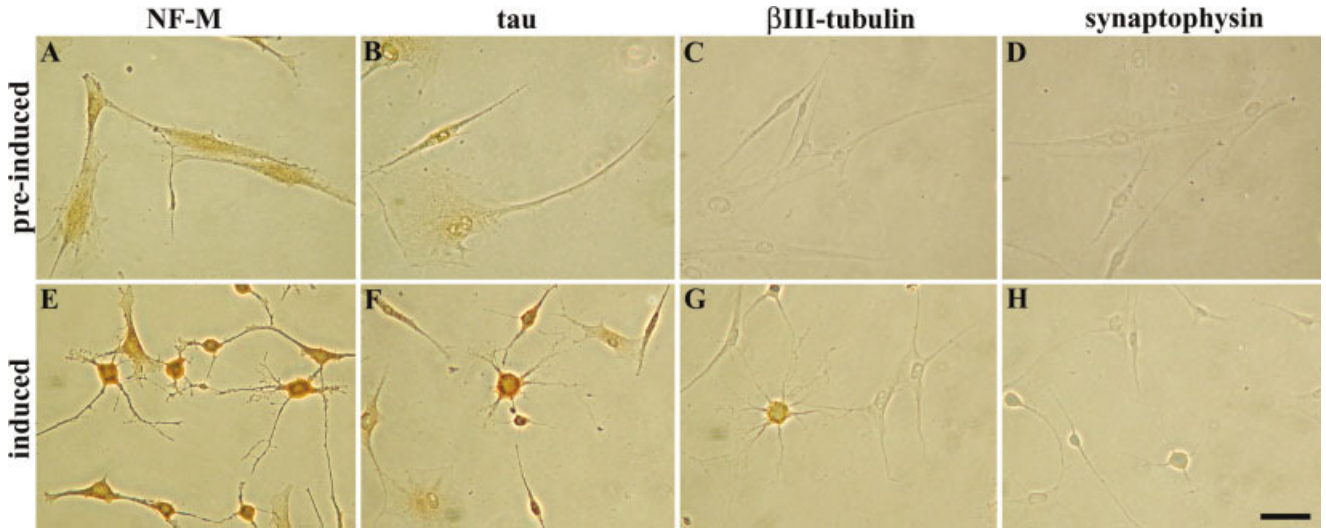

Fig. 8. Selective neuronal markers are present in MSC. Immunostaining of preinduced (**A–D**) and 24-hr-induced (**E–H**) MSC cultures. NF-M immunostaining is present in the cytoplasm of preinduced and induced MSC. Staining in cells with fibroblastic morphology is lighter compared with staining in neuron-like cells (A,E). A similar pattern of immunostaining is visible for tau (B,F). No βIII-tubulin immunolabel is present in preinduced MSC (C). After addition of induction medium, a small percentage of neuron-like cells is labeled for βIII-tubulin (G). No immunolabeling for synaptophysin is visible in preinduced or induced MSC (D,H). Scale bar = 50 μm.

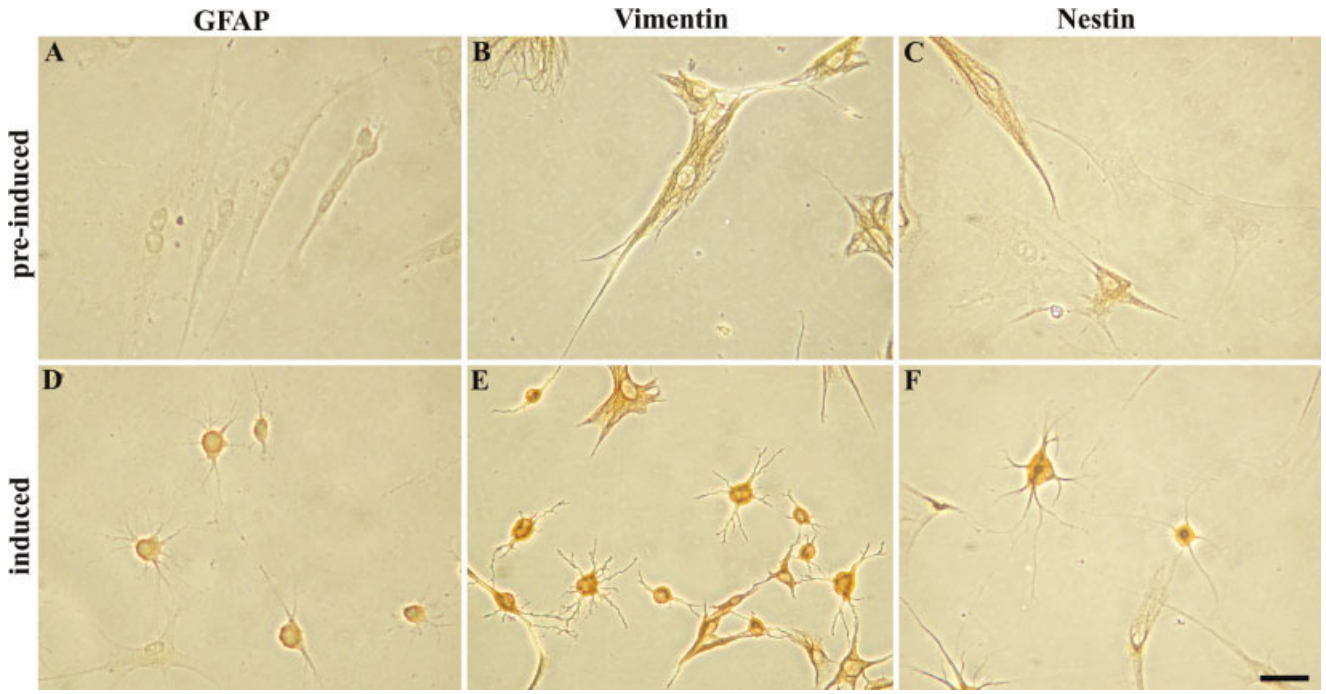

Fig. 9. Markers for glia, fibroblasts, and early neural stem cells are present in MSC. Immunostaining of preinduced (**A–C**) and 24-hr-induced (**D–F**) MSC cultures. Preinduced MSC are not labeled for GFAP (A); the cytoplasm of neuron-like cells in induced MSC cultures is GFAP positive (D). A filamentous vimentin immunolabel is visible in the cytoplasm of preinduced and induced MSC (B,E). Immunostaining for nestin is present in a subpopulation of cells in preinduced and induced MSC (C,F). Scale bar = 50 μm.

TABLE I. Transcript Levels Change Following Neuronal Induction*

	Copies per reaction 100 ng total RNA			Copies per reaction 100 ng total RNA			Copies per 1 ng poly-A^+ brain RNA
	Control MSC	Induced MSC	-Fold change	Control FB	Induced FB	-Fold change	
Vimentin	60,070 ± 8,062	40,440 ± 8,149	1.5-Fold decrease	130,200 ± 3,624	11,320 ± 1,874	11.5-Fold decrease	8,340 ± 1,392
βIII-Tubulin	5 ± 0.6	68 ± 26	14-Fold increase	59 ± 13	70 ± 21	1.2-Fold increase	8,880 ± 620
NF-M	3.3 ± 0.5	167 ± 17	51-Fold increase	121 ± 6	223 ± 31	1.9-Fold increase	33,690 ± 1,198

*Quantitative RT-PCR of RNA isolated from control or treated MSC or fibroblasts (FB) shows that transcript levels for vimentin, βIII-tubulin, and NF-M change after induction. Number of transcripts detected in each RT PCR reaction (mean of triplicate ± S.D.) and fold change in transcript level after induction.

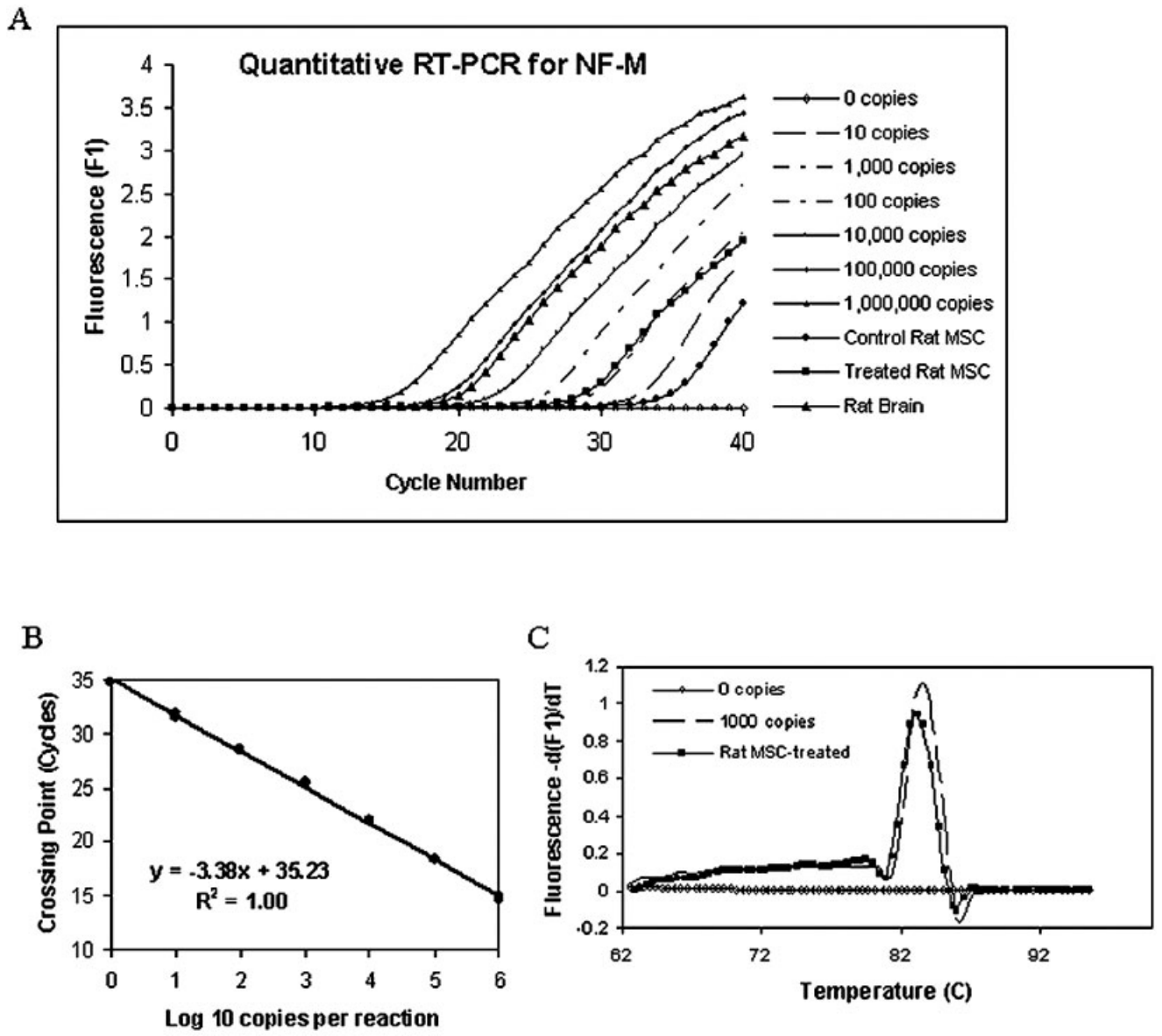

Fig. 10. Transcript levels change following neuronal induction. Quantitative RT-PCR of RNA isolated from control or treated MSC shows that transcript levels for vimentin, βIII-tubulin, and NF-M change after induction. **A:** Real-time amplification plot of NF-M cDNA standards from 100,000 to 0 copies per reaction and of RNA samples (100 ng) from control MSC, and induced MSC. As a positive control, 1 ng poly-A RNA isolated from rat brain was used as a template. Each standard was run in duplicate, and each sample was run in triplicate; for clarity only one plot of each is shown. **B:** Standard curve showing the correlation between $\log_{10}$ NF-M standard concentration and crossing point cycle number. **C:** Melting peaks for PCR products from NF-M cDNA standard and induced MSC sample are coincident suggesting that the same amplicon was produced. No such melting peak is observed in a sample with water as the template.

fined as a change in the gene expression pattern of a cell committed to the gene expression pattern of a different cell type (Liu and Rao, 2003). Transdifferentiation may lead in one step to a new phenotype, or, alternatively, an initial dedifferentiation event may be required. This process is not uncommon in the plant and animal kingdoms; limb regeneration in newts is accomplished through the transdifferentiation of differentiated cells of both ectodermal and mesodermal origin (Stocum, 2002). An alternative explanation of the detection of neuronal and glial cells of MSC origin in cell-transplantation studies is the possibility of a fusion event, including donor mesenchymal cells and host neurons or glia (for review see Jin and Greenberg, 2003; Liu and Rao, 2003).

Some studies have focused on the multipotency of MSC, showing that they can express genes from all three embryonic layers and the germline (Tremain et al., 2001; Woodbury et al., 2002; Seshi et al., 2003). The presence in undifferentiated MSC of the intermediate filament protein nestin, a marker of neuronal precursors (Sanchez-Ramos et al., 2000), is suggestive of the potential of MSC for neuronal differentiation.

Equally, treatment of cultured MSC with RA and cytokines resulted in neuronal differentiation of a small percentage of cells (Sanchez-Ramos et al., 2000). RA has been found to differentiate embryonic stem cells and embryonic carcinoma cells into neurons, probably via regulation of specific RA-responsive genes (Spinella et al., 2003). Several transplantation studies have shown the differentiation of a small percentage of MSC into neurons and glia in vivo (for review see Corti et al., 2003). This opens the possibility that a subpopulation of MSC may be able to adopt different fates. The seeming ability of culture-expanded mesenchymal MAPC to differentiate to endodermal and ectodermal as well as mesenchymal lineages (Reyes and Verfaillie, 2001) suggests that a subpopulation of early progenitors may exist within certain MSC cultures. The extent to which such progenitors, MSC, or HSC are responsible for the cell fates observed subsequent to the transplantation of unmanipulated bone marrow remains unresolved (for review see Herzog et al., 2003). In some cases, cell fusion is emerging as the most likely explanation (Terada et al., 2002; Ying et al., 2002; Alvarez-Dolado et al., 2003; Wehner et al., 2003).

The multipotency of MSC may also be enhanced by in vitro culture conditions, in a manner similar to that seen when embryoid bodies are treated with bFGF. In such cultures, small numbers of cells differentiated into neurons and glia as soon as bFGF was withdrawn (Okabe et al., 1996; Brustle et al., 1999). Could preconditioning regiments result in loss of patterning information and in the acquisition of a broader developmental potential? A recent study showed that treatment of bone marrow cells with different combinations of growth factors and RA induced a neuronal phenotype; however, the intracellular distribution of neural proteins was distinct from that of genuine neurons (Jin et al., 2003). Thus, the extent to which MSC may be able to transdifferentiate into mature, functional neurons remains unknown.

In conclusion, we do not dispute that MSC may exhibit multipotential properties beyond differentiation into mesenchymal lineages. Bone marrow, or other tissues, may contain a small population of early precursor cells that can differentiate into tissues other than those originating from mesoderm. In addition, treatment of MSC with physiological factors known to drive differentiation may well result in transdifferentiation or dedifferentiation followed by neural differentiation of MSC. However, it seems unlikely that in vitro exposure of MSC to DMSO and similar reagents will result in the transdifferentiation of MSC into cells with the morphologic attributes and functional qualities of mature neurons.

ACKNOWLEDGMENTS

We thank Maria Obrocka for assistance with tissue culture and Dr. B. Tim Himes for critically reviewing the manuscript. The antibody for vimentin (40E-C; developed by A. Alvarez-Buylla) was obtained from the Developmental Studies Hybridoma Bank maintained by the University of Iowa Department of Biological Sciences. L.H., L.K., and A.M. are supported by NIST Advanced Technology Program cooperative agreement 70NANH3017.

REFERENCES

Akiyama Y, Radtke C, Kocsis JD. 2002. Remyelination of the rat spinal cord by transplantation of identified bone marrow stromal cells. J Neurosci 22:6623–6630.

Alvarez-Dolado M, Pardal R, Garcia-Verdugo JM, Fike JR, Lee HO, Pfeffer K, Lois C, Morrison SJ, Alvarez-Buylla A. 2003. Fusion of bone-marrow-derived cells with Purkinje neurons, cardiomyocytes and hepatocytes. Nature 425:968–973.

Bang YJ, Pirnia F, Fang WG, Kang WK, Sartor O, Whitesell L, Ha MJ, Tsokos M, Sheahan MD, Nguyen P, Nikliaski WT, Myers CE, Trepel JB. 1994. Terminal neuroendocrine differentiation of human prostate carcinoma cells in response to increased intracellular cyclic AMP. Proc Natl Acad Sci USA 91:5330–5334.

Black MM, Slaughter T, Moshiach S, Obrocka M, Fischer I. 1996. Tau is enriched on dynamic microtubules in the distal region of growing axons. J Neurosci 16:3611–3619.

Brustle O, Jones KN, Learish RD, Karram K, Choudhary K, Wiestler OD, Duncan ID, McKay RD. 1999. Embryonic stem cell-derived glial precursors: a source of myelinating transplants. Science 285:754–756.

Chopp M, Li Y. 2002. Treatment of neural injury with marrow stromal cells. Lancet 1:92–100.

Corti S, Locatelli F, Strazzer S, Guglieri M, Comi GP. 2003. Neuronal generation from somatic stem cells: current knowledge and perspectives on the treatment of acquired and degenerative central nervous system disorders. Curr Gene Ther 3:247–272.

Cox ME, Deeble PD, Lakhani S, Parsons SJ. 1999. Acquisition of neuroendocrine characteristics by prostate tumor cells is reversible: implications for prostate cancer progression. Cancer Res 59:3821–3830.

Darling D, Tavassoli M, Linskens MH, Farzaneh F. 1989. DMSO induced modulation of c-myc steady-state RNA levels in a variety of different cell lines. Oncogene 4:175–179.

Deng W, Obrocka M, Fischer I, Prockop DJ. 2001. In vitro differentiation of human marrow stromal cells into early progenitors of neural cells by conditions that increase intracellular cyclic AMP. Biochem Biophys Res Commun 282:148–152.

Edson K, Weisshaar B, Matus A. 1993. Actin depolymerization induces process formation on MAP2-transfected non-neuronal cells. Development 117:689–700.

Giulian D, Baker TJ. 1986. Characterization of ameboid microglia isolated from developing mammalian brain. J Neurosci 6:2163–2178.

Herzog EL, Chai L, Krause DS. 2003. Plasticity of marrow derived stem cells. Blood 102:3483–3493.

Hofstetter CP, Schwarz EJ, Hess D, Widenfalk J, El Manira A, Prockop DJ, Olson L. 2002. Marrow stromal cells form guiding strands in the injured spinal cord and promote recovery. Proc Natl Acad Sci USA 99:2199–2204.

Isom HC, Secott T, Georgoff I, Woodworth C, Mummaw J. 1985. Maintenance of differentiated rat hepatocytes in primary culture. Proc Natl Acad Sci USA 82:3252–3256.

Jiang Y, Vaessen B, Lenvik T, Blackstad M, Reyes M, Verfaillie CM. 2002. Multipotent progenitor cells can be isolated from postnatal murine bone marrow, muscle, and brain. Exp Hematol 30:896–904.

Jiang Y, Henderson D, Blackstad M, Chen A, Miller RF, Verfaillie CM. 2003. Neuroectodermal differentiation from mouse multipotent adult progenitor cells. Proc Natl Acad Sci USA 100(Suppl 1):11854–11860.

Jin K, Greenberg DA. 2003. Tales of transdifferentiation. Exp Neurol 183:255–257.

Jin K, Mao XO, Batteur S, Sun Y, Greenberg DA. 2003. Induction of neuronal markers in bone marrow cells: differential effects of growth factors and patterns of intracellular expression. Exp Neurol 184:78–89.

Kim BJ, Seo JH, Bubien JK, Oh YS. 2002. Differentiation of adult bone marrow stem cells into neuroprogenitor cells in vitro. Neuroreport 13:1185–1188.

Kimhi Y, Palfrey C, Spector I, Barak Y, Littauer UZ. 1976. Maturation of neuroblastoma cells in the presence of dimethylsulfoxide. Proc Natl Acad Sci USA 73:462–466.

Kohyama J, Abe H, Shimazaki T, Koizumi A, Nakashima K, Gojo S, Taga T, Okano H, Hata J, Umezawa A. 2001. Brain from bone: efficient "meta-differentiation" of marrow stroma-derived mature osteoblasts to neurons with Noggin or a demethylating agent. Differentiation 68:235–244.

Koksoy S, Phipps AJ, Hayes KA, Mathes LE. 2001. SV40 immortalization of feline fibroblasts as targets for MHC-restricted cytotoxic T-cell assays. Vet Immunol Immunopathol 79:285–295.

Kopen GC, Prockop DJ, Phinney DG. 1999. Marrow stromal cells migrate throughout forebrain and cerebellum, and they differentiate into astrocytes after injection into neonatal mouse brains. Proc Natl Acad Sci USA 96:10711–10716.

Lennon DP, Haynesworth SE, Young RG, Dennis JE, Caplan AI. 1995. A chemically defined medium supports in vitro proliferation and maintains the osteochondral potential of rat marrow-derived mesenchymal stem cells. Exp Cell Res 219:211–222.

Liu Y, Rao MS. 2003. Transdifferentiation—fact or artifact. J Cell Biochem 88:29–40.

Mackay AM, Beck SC, Murphy JM, Barry FP, Chichester CO, Pittenger MF. 1998. Chondrogenic differentiation of cultured human mesenchymal stem cells from marrow. Tissue Eng 4:415–428.

McBurney MW, Jones-Villeneuve EM, Edwards MK, Anderson PJ. 1982. Control of muscle and neuronal differentiation in a cultured embryonal carcinoma cell line. Nature 299:165–167.

Mujtaba T, Han SS, Fischer I, Sandgren EP, Rao MS. 2002. Stable expression of the alkaline phosphatase marker gene by neural cells in culture and after transplantation into the CNS using cells derived from a transgenic rat. Exp Neurol 174:48–57.

Munoz-Elias G, Woodbury D, Black IB. 2003. Marrow stromal cells, mitosis, and neuronal differentiation: stem cell and precursor functions. Stem Cells 21:437–448.

Okabe S, Forsberg-Nilsson K, Spiro AC, Segal M, McKay RD. 1996. Development of neuronal precursor cells and functional postmitotic neurons from embryonic stem cells in vitro. Mech Dev 59:89–102.

Pittenger MF, Mackay AM, Beck SC, Jaiswal RK, Douglas R, Mosca JD, Moorman MA, Simonetti DW, Craig S, Marshak DR. 1999. Multilineage potential of adult human mesenchymal stem cells. Science 284:143–147.

Reyes M, Verfaillie CM. 2001. Characterization of multipotent adult progenitor cells, a subpopulation of mesenchymal stem cells. Ann N Y Acad Sci 938:231–233.

Sanchez-Ramos J, Song S, Cardozo-Pelaez F, Hazzi C, Stedeford T, Willing A, Freeman TB, Saporta S, Janssen W, Patel N, Cooper DR, Sanberg PR. 2000. Adult bone marrow stromal cells differentiate into neural cells in vitro. Exp Neurol 164:247–256.

Santos NC, Figueira-Coelho J, Martins-Silva J, Saldanha C. 2003. Multidisciplinary utilization of dimethyl sulfoxide: pharmacological, cellular, and molecular aspects. Biochem Pharmacol 65:1035–1041.

Sawai M, Takase K, Teraoka H, Tsukada K. 1990. Reversible G1 arrest in the cell cycle of human lymphoid cell lines by dimethyl sulfoxide. Exp Cell Res 187:4–10.

Seshi B, Kumar S, King D. 2003. Multilineage gene expression in human bone marrow stromal cells as evidenced by single-cell microarray analysis. Blood Cells Mol Dis 31:268–285.

Spinella MJ, Kerley JS, White KA, Curtin JC. 2003. Retinoid target gene activation during induced tumor cell differentiation: human embryonal carcinoma as a model. J Nutr 133:273S–276S.

Stocum DL. 2002. Development. A tail of transdifferentiation. Science 298:1901–1903.

Terada N, Hamazaki T, Oka M, Hoki M, Mastalerz DM, Nakano Y, Meyer EM, Morel L, Petersen BE, Scott EW. 2002. Bone marrow cells adopt the phenotype of other cells by spontaneous cell fusion. Nature 416:542–545.

Terasawa T, Miura Y, Masuda R. 1981. The mechanisms of the action of DMSO on the heme synthesis of quail embryo yolk sac cells. Exp Cell Res 133:31–37.

Tremain N, Korkko J, Ibberson D, Kopen GC, DiGirolamo C, Phinney DG. 2001. MicroSAGE analysis of 2,353 expressed genes in a single cell-derived colony of undifferentiated human mesenchymal stem cells reveals mRNAs of multiple cell lineages. Stem Cells 19:408–418.

Wehner T, Bontert M, Eyupoglu I, Prass K, Prinz M, Klett FF, Heinze M, Bechmann I, Nitsch R, Kirchhoff F, Kettenmann H, Dirnagl U, Priller J. 2003. Bone marrow-derived cells expressing green fluorescent protein under the control of the glial fibrillary acidic protein promoter do not differentiate into astrocytes in vitro and in vivo. J Neurosci 23:5004–5011.

Woodbury D, Schwarz EJ, Prockop DJ, Black IB. 2000. Adult rat and human bone marrow stromal cells differentiate into neurons. J Neurosci Res 61:364–370.

Woodbury D, Reynolds K, Black IB. 2002. Adult bone marrow stromal stem cells express germline, ectodermal, endodermal, and mesodermal genes prior to neurogenesis. J Neurosci Res 69:908–917.

Ying QL, Nichols J, Evans EP, Smith AG. 2002. Changing potency by spontaneous fusion. Nature 416:545–548.